

Fatigue wear of polyamides with surface defects under different loading conditions

Ahmed Abdelbary* and Mohamed N. A. Nasr^a

Department of Mechanical Engineering, Faculty of Engineering, Alexandria University, Egypt

(Received August 25, 2016, Revised November 27, 2016, Accepted November 28, 2016)

Abstract. Compared to metal-to-metal tribology, polymer tribology presents further complexity as it is more prone to be influenced by operating conditions. Over the past two decades, progress in the field of wear of polymers has led to the establishment of more refined wear mechanisms. The current paper establishes the link between different load parameters and the wear rate of polymers, based on experimental investigations. A pin-on-plate reciprocating tribometer was used to examine the wear behaviour of polyamide sliding against a steel counterface, under constant and fluctuating loads, in dry conditions. In addition, the influence of controlled imperfections in the polymer surface upon its wear rate were examined, under cyclic and steady loading, in order to better understand surface fatigue wear of polymers. The imposed imperfections consisted of vertical artificial deep crack (slit) perpendicular or parallel to the direction of sliding. The study concludes with the followings findings; in general, wear of polymers shows a significant tendency to the type of applied load. Under cyclic loads, polymers show an increase in wear rate compared to those tested under static loads. Such increase was found to increase with the increase in cyclic load frequency. It is also demonstrated that surface cracks results in higher wear rates, particularly under cyclic loads.

Keywords: tribology; wear; polymers; surface defects

1. Introduction

Recently, polymers have been increasingly used in numerous tribological applications. Wear characteristics of polymers encounter high degree of complexity; they not only may largely vary between different types of polymers, but they may also experience large variation for the same polymer under different loading conditions. This is mainly because the wear characteristics of polymers are sensitive to a multitude of factors. For sliding wear, these factors mainly include; applied load, contact pressure, relative speed, surrounding media, and the characteristics of rubbing surfaces. Out of the aforementioned factors, the current manuscript focuses on the effects of load type, cyclic versus steady, and surface defects on the wear characteristics of polymers.

Examination of the effects of different cyclic-load parameters on the wear behaviour of nylon 66 showed a significant increase in wear rate under cyclic loading compared to static loading. It

*Corresponding author, Ph.D., E-mail: elbary1972@yahoo.com

^aAssistant Professor, E-mail: mohamednasr@alexu.edu.eg

was reported that a direct relation between load-ratio and wear rate, as well as load frequency and wear rate (Abdelbary *et al.* 2014). This has been mainly attributed to fatigue wear mechanisms, where cycling loading has two major effects; first, the loading-unloading cycle is responsible for creating highly stressed subsurface regions which, in turn, initiate subsurface micro cracks that eventually grow during the loading portion of each cycle. Subsurface crack propagation accelerates the failure and removal of surface material from the highly stressed polymer peaks, hence greatly increasing the wear rate. Second, thermal loading effects, which depend on loading frequency, alter the dynamic mechanical properties of bulk material, where thermal softening results in higher wear rates (Yap *et al.* 2002, Smata *et al.* 2010, Juliana *et al.* 2013).

The nature, whether surface or subsurface, and number of crack initiation sites in the near-surface layer depend on the type of loading and sliding conditions (for example, rolling versus sliding, temperature, pressure, humidity). As an example, cracks evolving under rolling conditions, which are typically used to study fatigue wear, tend to be more macroscopic or coarser than those under sliding conditions (Shi *et al.* 2014). However, the insufficient details as how to crack initiation and propagation occur, as well as their accompanied microstructural changes, could not constitute a foundation for a comprehensive understanding of such mechanisms.

Microscopic studies (Cooper *et al.* 1993, Pei *et al.* 2016) of polyethylene wear specimens and acetabular cups showed evidence that, localized macroscopic wear mechanisms are extremely important in the wear of ultra-high-molecular-weight-polyethylene (UHMWPE). As the hip joint is subjected to cyclic loading, where the direction and magnitude of friction force varies, this results in cyclic stress fields in the macroscopic asperity peaks of the polymer surface, and eventually surface and subsurface crack formation and propagation. This fatigue process is likely to lead to delamination and to an increased wear rate, as crack propagation accelerates material removal. Material removal from one part of the contact surface results in increased stresses in adjacent areas, and subsequent higher plastic shear strains. Similar observations were reported in an *in vivo* study of wear mechanisms in highly cross-linked UHMWPE (Letita *et al.* 2004, Daniel *et al.* 2016), where such mechanisms were also compared to predictions based on *in vitro* wear testing. In (Daniel *et al.* 2016), all tested polyethylene acetabular liners experienced surface cracking, abrasion, pitting and scratching. These findings were clearly different from those observed in hip-simulators, which demonstrated only surface scratches. Such discrepancy is mainly attributed to the differences between *in vivo* and *in vitro* studies in the associated lubrication conditions and cyclic-load parameters.

The current paper focuses on the influence of different load parameters on fatigue wear of polymers, based on experimental investigations. The effects of load ratio and frequency on wear rate are examined, and compared to wear rates obtained under steady loads that correspond to the mean values of cyclic loading. In addition, the relative change in wear rate due to pre-existing surface cracks is discussed, in an effort to provide a better understanding of surface fatigue wear.

2. Materials and methods

2.1 Wear specimens and counterface

As it is widely used in different mechanical applications, polyamide 66 (PA66) has been selected as the target material for the current work. The material was manufactured by *Rochling Plastics, USA*, under the trade name of *Sustamide 66*. Cylindrical pins with a diameter of 8 mm

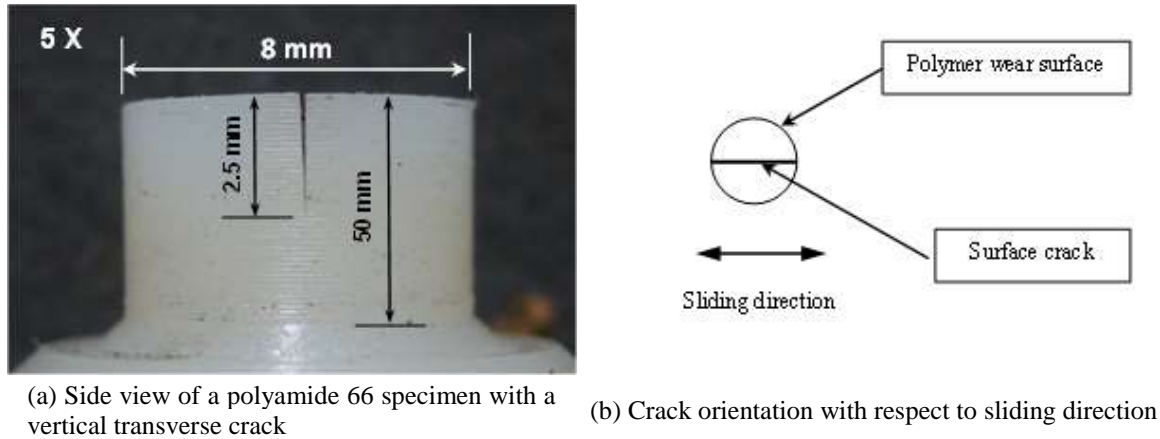


Fig. 1 Wear Specimen

were used, which were machined from 14-mm solid bars, Fig. 1(a). The selected pin diameter, along with the used sliding speed and applied load, ensured having a Pv value that is well below the Pv limit of the material, which is $90 \cdot 10^{-3}$ N/(m.s) (Laurence 2016). A metallic counterface made of AISI 1050 steel, with dimensions of $330 \times 30 \times 3$ mm, were used in all experiments. The plates were prepared by surface grinding, in the sliding (longitudinal) direction, in order to have a centre-line average roughness (R_a) of $0.2 - 0.4 \mu\text{m}$. In order to examine the effects of surface cracks; artificial, central, transverse, surface cracks were introduced using a sharp razor, as shown in Fig. 1(a). The crack has a nominal height of 2.5 mm, and was aligned perpendicular to the sliding direction, as illustrated in Fig. 1(b). The polymer specimens had an initial surface roughness of $1.5 \mu\text{m } R_a$.

2.2 Tribometer

Fig. 2 shows a schematic of the used tribometer, which was designed to provide a reciprocating motion with a speed of 0.25 m/s. This speed, along with other load parameters, ensured having a Pv value that is well below the Pv limit of the material, as mentioned earlier. The tribometer has twelve wear tracks (not shown); six for constant loading and six for cyclic loading. The load parameters, except sliding speed, of each track were controlled independently. The temperature of the counterface was measured during testing, using thermocouples, in order to ensure that temperature does not exceed the glass transition temperature of the polymer.

The test rig was designed to be able to provide a reciprocating motion to the matting counterface at a linear constant speed for most of its stroke. The metallic counterfaces were mounted on a reciprocating carriage. A special chain drive mechanism was designed to generate the acquired reciprocating motion to the carriage with a constant linear speed. The polymer wear pins were held vertically in contact with the metallic counterface while the loads were applied normally to the top of the pin holder. The cyclic loading was provided by an eccentric circular cam spring system while the constant applied loads were provided by dead weights. The detailed design of the used tribometer could be found in (Abdelbary 2014).

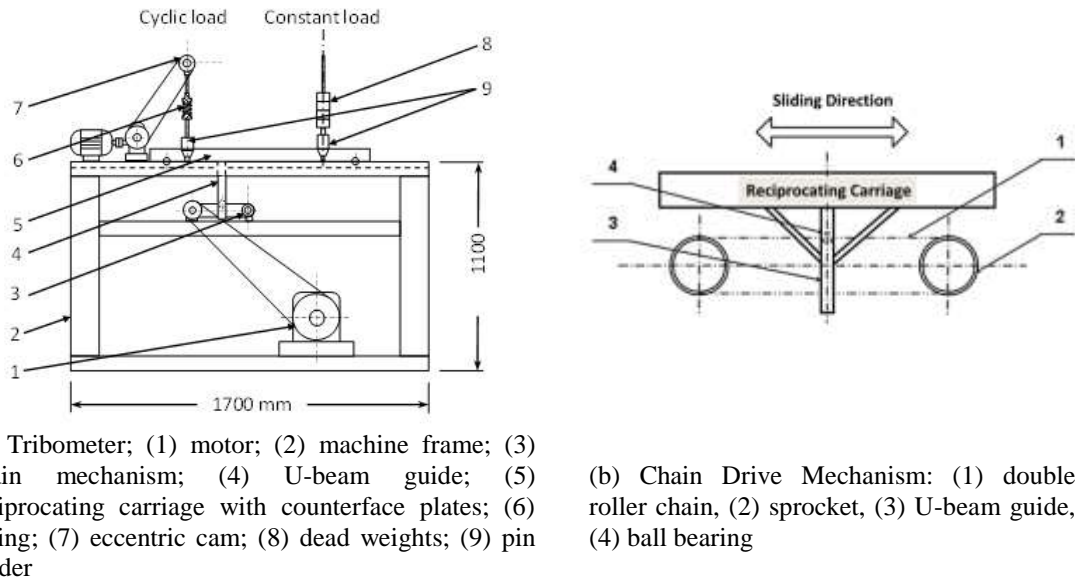


Fig. 2 Schematic of the used tribometer

2.3 Test matrix

In order to assess the effects of cyclic load frequency, magnitude of static load, and surface cracks on the wear rate of PA66, a total of ten tests were performed; five for steady loading and five for cyclic loading. Table 1 and Table 2 present the test matrix for static and cyclic loading, respectively. All tests were performed in dry non-lubricated conditions. In order to examine the effects of surface cracks, two cases were considered. A case with a single central crack, shown in Fig. 1(a), and another with three parallel cracks, in order to examine the effects of multiple surface defects. The case with three cracks has one central crack, and one crack on each side, with 1-mm spacing in between. In order to be able to compare cyclic-load results to steady-load results, static loads equal to the mean values, F_{mean} , of cyclic loads were used. All cyclic-load testing was performed using a load ratio (minimum to maximum load ratio: $F_{\text{min}}/F_{\text{max}}$) of 0.06, which represents a case of repeated loading.

3. Results

3.1 Wear Rate (WR)

In order to find out the wear rate, WR , the worn volume, V (mm^3), was plotted against the sliding distance, X (m); the slope of the curve (straight line) represents the wear rate. The worn volume was calculated based on the measured dimensions of worn specimens. Fig. 3 presents the wear graph of test (5), as an example of the obtained results. Measurements were performed every 10 km. As shown, wear graphs possessed two straight-line regions, the first represents the running-in period and the second represents steady-state wear. Table 1 and Table 2 present the steady-state

wear rates obtained under different static and cyclic loads, respectively. Results postulated that wear rates are significantly affected by load type and surface cracks. It is important to note that, the maximum recorded surface temperature during all tests was found to be 42 - 44°C, which is lower than the glass transition temperature of PA66 (57°C) (Röchling®). Accordingly, sever wear due to mechanical degradation did not take place in the current work.

Under static loading, an increase in load resulted in higher wear rates. This was more significant in the presence of a surface crack. At the same time, at a constant load, a surface crack resulted in higher wear rates; this was more evident at higher loads. In other words, the effects of surface defects become more significant as the load increase. Finally, the increase in the number of surface cracks resulted in a significant increase in wear rate.

Under cyclic loading, an increase in load frequency resulted in higher wear rates, especially in the presence of a surface crack. At the same time, surface cracks resulted in higher wear rates; this was more significant at higher cyclic frequencies. Similar to static loading, and increase in the number of surface cracks resulted in higher wear rates; however, this was less evident under cyclic loading.

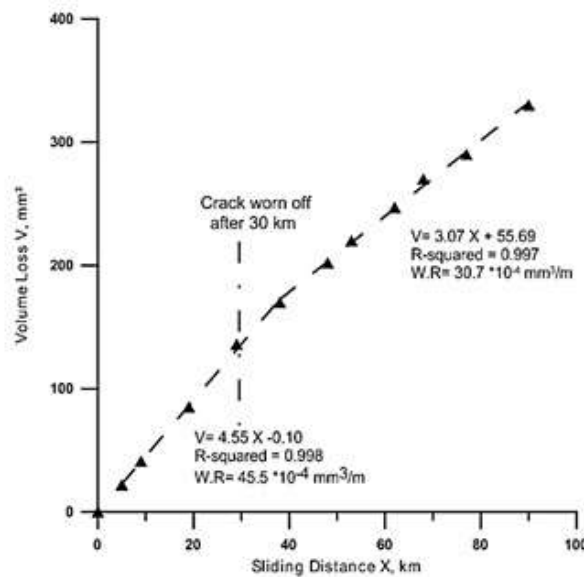


Fig. 3 Volume loss (V) against sliding distance (X), test (5)

Table 1 Results of constant load wear tests

Test	Applied force “F” (N)	Number of surface cracks	Total sliding distance “X” (km)	Wear rate “WR” × 10 ⁻⁴ (mm ³ .m ⁻¹)
1	90	-	110	13.3
2	90	1	80	14.8
3	90	3	80	25.2
4	135	-	90	18.1
5	135	1	90	30.7

Table 2 Results of cyclic load wear tests ($F_{\text{mean}}=90$ N, load ratio ($F_{\text{min}}/F_{\text{max}}=0.06$)

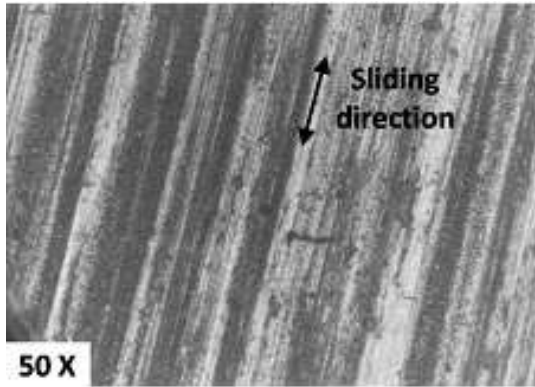
Test	Cyclic frequency " f " (Hz)	Number of surface cracks	Total sliding distance " X " (km)	Wear rate " WR " $\times 10^{-4}$ ($\text{mm}^3 \cdot \text{m}^{-1}$)
6	0.25	-	80	13.7
7	0.25	1	80	21.8
8	0.25	3	80	29.7
9	1.50	-	100	15.8
10	1.50	1	80	30.1

3.2 Optical microscopy

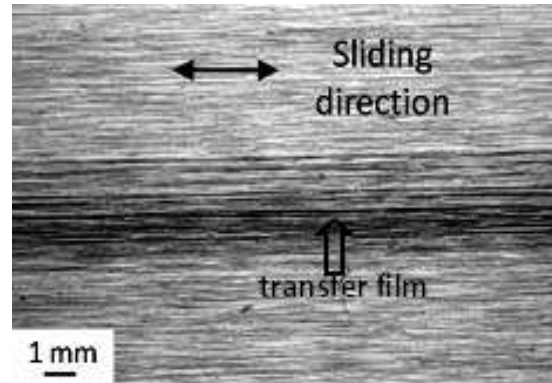
Typical sliding-wear features were observed on the worn surfaces of all specimens. In general, surface roughness was found to drop with sliding distance. At the beginning of testing, specimens had an average surface roughness of $1.5 \mu\text{m} R_a$ (machined surface) and as the test progressed, the original surface was replaced by a smoother one, which had an average surface roughness of $0.85 \mu\text{m} R_a$ during the running-in period and $0.6 \mu\text{m} R_a$ during the steady-state period.

Fig. 4(a) shows the worn surface of an un-cracked specimen under cyclic loading ($f=1.5$ Hz), test (9), generated after 60 km. Wear grooves parallel to the sliding direction were evident, and were present at all stages. These grooves can be attributed to banded material transfer to the counterface, eventually forming a transfer film. The steel counterface was examined regularly, in order to study the formation and build-up of polymer transfer film. Fig. 4(b) shows a uniform and continuous transfer film on the counterface, after 20 km of sliding during test (9). Polymer transfer was found to be maximum along the centreline of the wear track, and decreases outwards. This is not surprising since the wear pin is circular, and hence the mid-track position comes into contact with a greater area of wear pin during each pass. The transfer film width was about 4 mm in the beginning, and then widened as the test progressed, eventually producing a fairly uniform appearance.

Fig. 5 shows the worn surface of a specimen with a single crack under static loading, test (2), during the running-in period (after 20 km). Wear grooves and pitting were observed on both sides of the crack mouth, and their appearance did not change during the test. Crack mouth opening was detected throughout the whole test duration. As the test runs, polymer wear debris were trapped and accumulated inside the crack, resulting in progressive crack opening. Fig. 5(b) shows wear debris of test (2). Fig. 6(a) shows the worn surface of a specimen with a single crack under cyclic loading, test (10), after 20 km. Fig. 6(b) shows the transfer film formation in test (10), which was different from un-cracked specimens. As shown, two parallel transfer film tracks were detected in the sliding direction. Each track was about 0.5 mm in width, and the two tracks were separated by a distance of about 1 mm. These tracks widened as the test progressed, till they finally merged by the end of running-in period producing a unique track of width equal to the diameter of test pin. Fig. 7(a) shows the worn surface of a specimen with three cracks under static loading, test (3), after 20 km. Compared to the case with a single crack, test (2), relatively dark and high density wear grooves, parallel to the sliding direction, were observed especially in the regions in between the cracks. The transfer film, Fig. 7(b), consisted of several transfer film tracks at the beginning of testing, which eventually merged and the film completely covered the wear track.

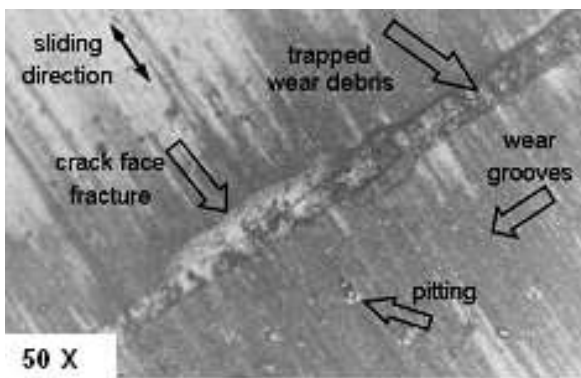


(a) wear pin surface after 60 km, showing wear grooves parallel to the sliding direction

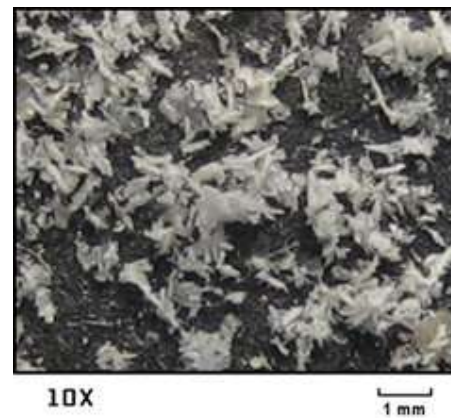


(b) steel counterface showing a transfer film formed after 20 km

Fig. 4 Test 9 optical micrographs

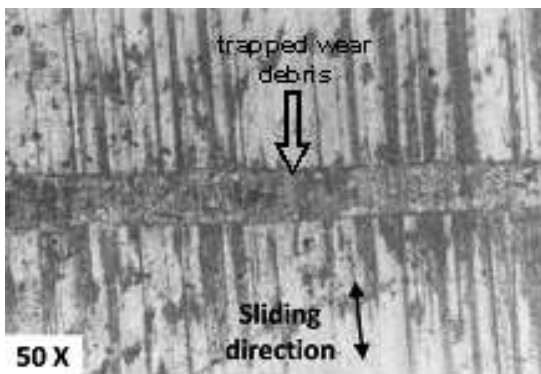


(a) rubbing surface with trapped wear debris

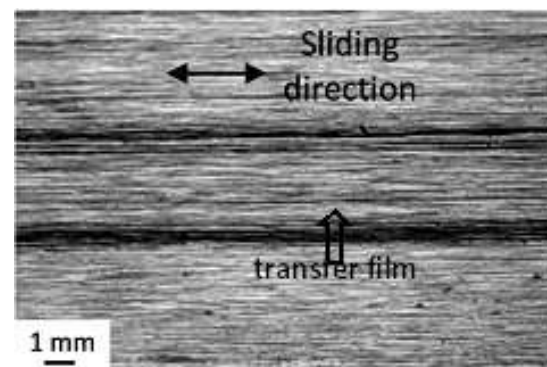


(b) wear debris

Fig. 5 Optical micrograph of test (2) after 20 km sliding



(a) wear pin surface with trapped wear debris inside the crack mouth



(b) steel counterface with transfer film formed

Fig. 6 Optical micrographs of test (10) after 20 km sliding

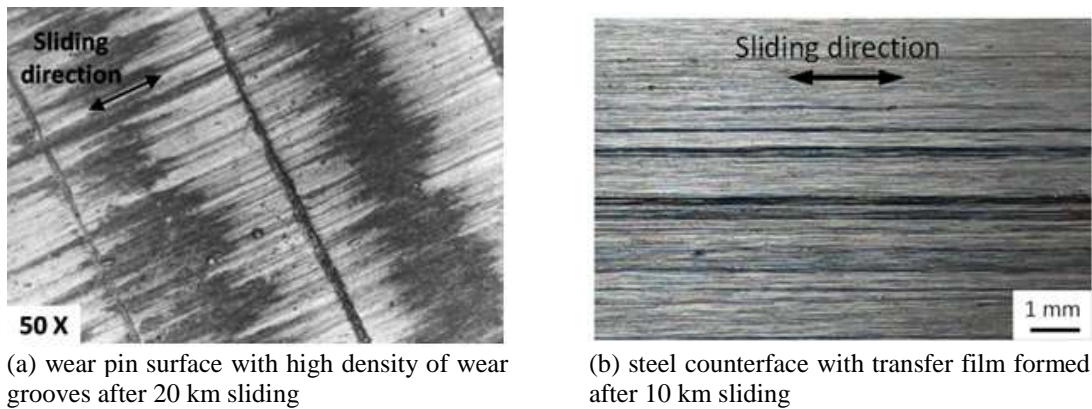


Fig. 7 Optical micrographs of test (3)

4. Discussion

The current results showed an increase in wear rate under cyclic loading compared to static loading. This has been also reported in (Abdelbary *et al.* 2014) for polymer-metal sliding systems, and has been attributed to fatigue wear. In fatigue wear, scratches and surface cracks play a major role in controlling the wear behaviour of polymers, in a more dominant way than they do under static loading, as have been widely reported in the literature (Barbour *et al.* 1995, Pei *et al.* 2016). This leads to a remarkable increase in wear rate, which may go up to two orders of magnitude greater than wear rates under static loading. As clearly shown in Fig. 8, cyclic load effects were found to be more evident at higher load frequencies; this was more significant in presence of surface cracks. Since higher loading frequencies result in a more significant increase in polymer temperature, which in turn leads to a drop in mechanical properties (Sadeghipour *et al.* 2013); this explains the current results. Higher frequencies resulted in higher temperatures, and heat build-up, which subsequently resulted in mechanical degradation of polymer properties, due to thermal softening effects, of the near surface layer. In the examined range, a linear relationship between load frequency and wear rate was found; however, a wider range of frequencies needs to be investigated for a more general conclusion.

The present work has demonstrated that surface cracks result in significantly higher wear rates, under static and dynamic loading, which agrees with previously published results (Fam *et al.* 1993, Sadeghipour *et al.* 2013). This was more evident under dynamic loading, and became more evident as the number of surface cracks increased, as can be seen in Fig. 8. The effect of the number of surface cracks is reflected in the density of wear grooves, as can be seen by comparing Fig. 7 to Fig. 5(a). As the number of cracks increase, the polymer surface suffers more unconformity leading to an increase in wear rate. The imposed surface cracks act as a nucleation site for subsurface crack formation. The subsurface cracks propagate and start to interconnect forming a network of sub-surface cracks, until eventually bulk polymer material separates as wear debris, and may also result in pitting and spalling, as shown in Fig. 5. Another important issue is that, during reciprocating sliding, the friction force tends to open the crack mouth, which helps wear debris to get trapped inside the crack. This results in an irregular surface that may well decrease the polymer/metal conformity, and hence would result in higher wear rate. During cyclic loading, the trapped debris tend to escape during the unloading phase of the load cycle, which results in higher

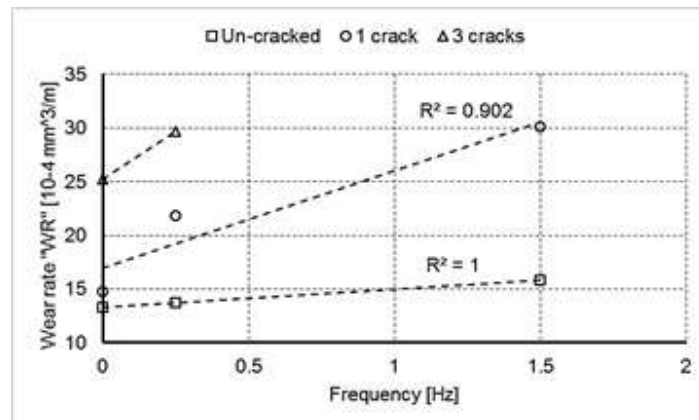


Fig. 8 Effect of loading frequency on wear rate of PA66 specimens, with and without surface cracks ($F_{\text{mean}}=90$ N). The case with zero frequency represents static loading

wear rate (Barbour *et al.* 1995). Wear occurs during the loading phase due to asperity interactions, but the debris are unable to escape due to the high surface conformity, as in the case of static loading. On the other hand, during the unloading phase, surface conformity decreases and wear debris become free to escape. It is worth mentioning that, although the length of the imposed artificial cracks (2.5 mm) was selected in order to ensure crack propagation, in fact, almost no crack propagation was detected during testing. This could be mainly attributed to elastic recovery, which typically takes place in relatively ductile polymers and makes it hard to detect crack propagation (Lamethe *et al.* 2003).

Even though, all imposed surface cracks were almost totally worn off by the end of the running-in period, cracked specimens showed different wear rates from the un-cracked ones during steady-state wear. Accordingly, it is believed that this phenomenon could be related to transfer film formation, which governs the wear behaviour during steady-state wear (Emerson *et al.* 2015). This is because, steady-state wear is influenced by two parameters; 1) the surface topography of the metallic counterface, and 2) the characteristics of the transfer film formed after running-in (Gregory *et al.* 2014, Jiabin *et al.* 2016). Studying reciprocating sliding wear of polyamide against a metallic counterface (Matthias *et al.* 2013) showed a correlation between the changes in transfer film geometry, during the running-in period, and the friction coefficient as well as wear rate. During running-in, the thickness of the transfer film increases with sliding time, until a maximum limiting value is reached. The limiting thickness is probably a characteristic feature of each rubbing pair, and operating variables. Transfer film formation is determined by the balance between the removing action of the front edge of the polymer body and the replenishment of the polymeric film by material transfer. Finally, since the arrangement of surface grooves in cracked pins was found to be different from those detected in un-cracked polymers, it is suggested that the polymer has transferred non-homogeneously to the counterface, unlike what happened with un-cracked specimens. Consequently, relative change in wear rate due to surface cracks is expected.

4. Conclusions

Based on the results presented in this study, the following conclusions were drawn with regards

to reciprocating sliding wear of polyamide.

(a) The wear behaviour of polyamide is highly affected by the presence of surface cracks and defects, where surface cracks result in higher wear rates. This is mainly because friction force acts on the crack mouth resulting in crack opening, which helps wear debris to get trapped inside the crack. This results in an irregular surface that may well decrease the polymer/metal conformity, and hence would result in higher wear rate. Such increase in wear rate becomes more significant as the number of cracks increase, and is more pronounced under cyclic loading conditions, compared to static loading.

(b) Compared to static loading, a repeated cyclic load with a mean value that is equal to the static load results in higher wear rate. This becomes more significant with the increase of cyclic frequency, as well as with the presence of surface cracks. The increase with cyclic frequency is attributed to thermal cycling effects, which leads to mechanical degradation of the polymer.

References

- Abdelbary, A. (2014), "Wear of polymers and composites", Woodhead Publishing, Oxford, ISBN 9781782421771, <http://dx.doi.org/10.1533/9781782421788.133>.
- Abdelbary, A., El Fahham, M.I. and Elnady, M.E. (2014), "Load dependent wear characteristics of polymer-metal sliding", *Proceeding of the 15th International Conference on Applied Mechanics and Mechanical Engineering AMME-15*, Military Technical College, Cairo, May.
- Barbour, P.S.M., Barton, D. and Fisher, J. (1995), "The influence of contact stress on the wear of UHMWPE for total replacement hip prostheses", *Wear*, **181-183**, 250-257.
- Cooper, J.R., Dowson, D. and Fisher, J. (1993), "Macroscopic and microscopic wear mechanisms in UHMWPE", *Wear*, **162-164**, 378-84.
- Daniel MacDonald, Anton, E.B. and Steven, M.K. (2016), *41- MicroCT analysis of wear and damage in UHMWPE*, In UHMWPE biomaterials handbook (Third Edition), William Andrew Publishing, Oxford, 786-796, ISBN 9780323354011, <http://dx.doi.org/10.1016/B978-0-323-35401-1.00041-7>.
- Emerson, E.N. and Andreas, A.P. (2015), "The effect of surface roughness on the transfer of polymer films under unlubricated testing conditions", *Wear*, **326-327**, 74-83.
- Fam, H., Keer, L.M., Chang, W. and Cheng, H.S. (1993), "Competition between fatigue crack propagation and wear", *J. Trib.*, **115**(1), 141-145.
- Gregory, Sawyer, Nicolas, Argibay, David, L. Burris and Brandon, A. Krick (2014), "Mechanistic studies in friction and wear of bulk materials", *Ann. Rev. Mat. Res.*, **44**, 395-427.
- Jiixin, Ye, David, L.B. and Ting, X. (2016), "A review of transfer films and their role in ultra-low-wear sliding of polymers", *Lubricants*, **4**(1), 4.
- Juliana Antonino de Souza, Liliane Canuto Dolavale and Sergio Alvaro de Souza Camargo (2013), "Wear mechanisms of dental composite restorative materials by two different in-vitro methods", *Mat. Res.*, **16**(2), 333-340.
- Lamethe, J.F., Sergot, P., Chateauminois, A. and Briscoe, B.J. (2003), "Contact fatigue behaviour of glassy polymers with improved toughness under fretting wear conditions", *Wear*, **255**, 758-765.
- Laurence WMcKeen (2016), *Polyamide plastics (Nylons)*, In Fatigue and Tribological Properties of Plastics and Elastomers (Third Edition), William Andrew Publishing, 199-260, ISBN 9780323442015, <http://dx.doi.org/10.1016/B978-0-323-44201-5.00008-3>.
- Letita, B., David, A. and Pruitt, L.A. (2004), "Wear and surface cracking in early retrieved highly cross-linked polyethylene acetabular liners", *J. Bone Joint Surg.*, **86-A** (6), 1271-1282.
- Matthias, S., Jeanette, K., Roman, B. and Tobias, H. (2013), "Running-in due to material transfer of lubricated steel/PA46 (aliphatic polyamide) contacts", *Wear*, **301**(1-2), 758-762.
- Pei, X.Q. and Friedrich, K. (2016), *Friction and wear of polymer composites*, In Reference Module in

Materials Science and Materials Engineering, Elsevier, ISBN 9780128035818,
<http://dx.doi.org/10.1016/B978-0-12-803581-8.03074-5>.

Röchling Engineering Plastics, USA, www.roechling-plastics.us

Sadeghipour, K., Baran, G., Zhang, H. and Wu, W. (2013), "Modeling of fatigue crack propagation during sliding wear of polymers", *J. Eng. Mater. Technol.*, ASME, **125**(2), 97-106.

Shi, X., Kida, K. and Kashima, Y. (2014), "Surface crack and wear of PPS polymer thrust bearings under rolling contact fatigue in water", *Mat. Res. Innov.*, **18**(5), 42-47.

Smata, L., Bouzid, S. and Azari, Z. (2010), "Damage by cyclic loading of composite dental materials", *Particle Contin. Aspect. Mesomech.*, doi:10.1002/9780470610794.ch65.

OP